Proceedings of the Canadian Society for Mechanical Engineering International Congress
32nd Annual Conference of the Computational Fluid Dynamics Society of Canada
Canadian Society of Rheology Symposium
CSME-CFDSC-CSR 2025
May 25–28, 2025, Montréal, Québec, Canada

Effect of EGR Direct-Injection on the Resulting Flow and Stratification in a Spark-Ignition Engine Using CFD

Baptiste Cunha*, Patrice Seers
Mechanical Engineering Department,
École de Technologie Supérieure, Montréal, Canada
*baptiste.cunha.1@ens.etsmtl.ca

Abstract—Exhaust gas recirculation (EGR) is widely implemented in internal combustion engines to reduce pollutant emissions. The traditional way of introducing EGR is by creating a homogeneous air-exhaust gas mixture in the engine intake system. In this paper a novel technique of EGR is studied numerically and is based on the direct injection of exhaust gases in the cylinder. Such an approach can create exhaust gases stratification which offers benefits compared to the traditional technique. To explore the capacity of the novel approach, 3D-CFD simulations were used. Results showed a high velocity EGR jet, emanating from the three EGR inlets, which crosses the cylinder and hits the junction piston-cylinder liner on the opposite side. The jet then continued its course creating a clear stratification of nitrogen inside the cylinder along the liner surface. Moreover, CFD results suggested a direct advantage of the proposed approach as a significant increase of turbulence (measured by TKE, turbulence intensity, and swirl ratio) is observed and persisted up to spark timing when compared to a homogeneous EGR approach.

Keywords-EGR stratification; exhaust gas direct injection; spark-ignition engine; computational fluid dynamics

I. INTRODUCTION

The transport sector has been known to be responsible for a large proportion of the greenhouse gas emissions [1] and as such significant reduction of pollutant emissions from vehicles is seen as a key factor in mitigating the risks associated with global warming. Consequently, technological research has intensified in recent years because internal combustion engines (ICEs) are still set to play a major role in the transport industry over the coming decades [2]. In this context, recent research has focused on reducing specific fuel consumption and cutting pollutant emissions, with a view to reducing their impact on the environment.

Exhaust gas recirculation (EGR) is a well-known technique to reduce nitrogen oxides (NO_x) emissions and has been widely implemented in ICEs. The technology was implemented in diesel engines as a way of controlling NO_x emission by lowering the temperature of the combustion chamber [3]. The use of homogeneous EGR in spark-ignition (SI) engines also offers other advantages such as a lower fuel consumption due to a decrease of intake charge losses at part loads [3]. EGR systems are traditionally designed for two distinct operating modes: internal and external. Internal EGR traps combustion gases inside the cylinder using valve overlap, while external EGR collects burnt gases in the exhaust system and supplies them to the intake charge via piping and a control valve driven by the ECU. In both cases, the turbulent mixing of the engine flow creates a homogeneous mixture of fresh gases and EGR.

The homogeneous EGR system has some limitation due to EGR mixture dilution, which is responsible for combustion instabilities or incompletion as well as lowering fuel conversion efficiency through heterogeneity of the EGR/air-fuel mixture [4]. In order to enhance the level of EGR dilution before combustion instability appearance, another approach has been pursued and consists in EGR stratification. EGR stratification involves creating at least two separate zones one with a high concentration of burnt gas, and another one with an air-fuel mixture. Research on EGR stratification has been mostly oriented into identifying potential in-cylinder stratification configuration as well as developing a way to implement stratification in engines. These subjects are thus shortly reviewed in what follows.

The positive effects of EGR stratification on a gasoline engine have been demonstrated in 1986 using tangential intake ports as to create a swirling EGR stratification near the cylinder walls [5]. The resulting swirling motion of the EGR allowed a higher EGR rate of 26% in comparison to 10%, for the homogeneous approach. Moreover, fuel economy was improved by 10%. Another approach to EGR stratification was named Combustion Control by Vortex Stratification (CCVS) [6] and consists at independently introducing EGR and the air-fuel mixture in the engine's cylinder through dedicated intake runners and ports to achieve stratification on the width of the tumble flow structure. A maximum EGR rate of 40% was

reached on particular operating points. However, no comparisons were carried out with a homogeneous EGR configuration [6-8].

Another technique achieved a three-zone stratification through the partition of the intake ports into three flow sections using flow adapters [9]. Nitrogen (N_2) was used to mimic EGR during the experiments. The resulting stratification consisted of an air-fuel mixture, at the center of the cylinder, and burnt gases on both sides. Flow adapter orientation generated a tumble of high intensity that sustained EGR stratification through the combustion process. Even though, a substantial performance improvement under stratification relative to the homogeneous case was reported, stratification was possible only on one operating point due to the presence of a swirling motion in the cylinder. Later, another three-zone stratification of EGR/air/air-fuel mixture was studied in a prechamber SI engine [10] with the particularity that stratification is confined to the prechamber volume. Initially residual burnt gas fill-up the prechamber while air entered the cylinder during the intake stroke. During the compression stroke, stratification of burnt gas and air is created in the prechamber where fuel is also injected. Hence, a three-zone stratification (EGR/air/air-fuel) is thus reach in the prechamber where the spark plug is also located. Results show a drastic reduction of HC and NO_x emissions by 60% and 20-40%, respectively at a EGR rate of 45%.

Radial EGR stratification was also studied with a SI engine by supplying exhaust gas to the intake port using a dedicated pipe [11]. To avoid EGR-air mixing in the intake port, deflectors separated both flows. The approach achieved EGR stratification by controlling temporally the amount air or EGR that entered the cylinder, thanks to valves. This approach resulted in higher EGR-rate along with a significant NO_x reduction when compared to the homogeneous case. Finally, EGR stratification was studied through the use of a solenoid valve controlling temporally the amount of EGR introduced in the intake port [12]. Different EGR injection strategies (timing and duration) were tested and it was reported that EGR stratification resulted in a shorter combustion duration.

In summary, different EGR stratification concepts have been demonstrated over the year and consisted in modifying the intake runners and ports so as to separate the exhaust gases from the air-fuel mixture and to achieve in-cylinder stratification. EGR stratification allows a higher rate of dilution than homogeneous EGR with similar or lower NO_x emissions and shorter combustion duration. However, by using the intake ports to achieve EGR stratification also signifies that EGR at high load is difficult to achieve and is detrimental to engine power. The proposed novel approach, studied numerically herein, does not have this limitation as EGR is introduced in the cylinder by going through the cylinder head and is thus named direct injection EGR. The objective of this paper is to quantify the consequence of using a direct injection approach on the in-cylinder flow, turbulence level and EGR stratification. To do so, a 3D-CFD model is developed.

II. NUMERICAL SETUP

A. Computational domain generation

The computational domain was created using reverse engineering techniques from an industrial CT scan of an air-cooled, single cylinder SI engine that has been modified to conduct experimentation as a proof of concept. The resulting cylinder head is illustrated in Fig. 1 and where the modification consists in adding three exhaust gas inlets to the cylinder head. The location and orientation were chosen by space availability and ease of installation in this first configuration thus, no optimization has been performed yet. Three inlets are necessary to attain significant EGR rates due to the maximum flow rate of the exhaust gas electronically control valves used experimentally. The engine main specifications are shown in Table I.

TABLE I. ENGINE SPECIFICATIONS

Engine type	Single cylinder, 4 stroke, air cooled
Displacement	389 cm^3
Bore × Stroke	88 mm × 64 mm
Connecting rod length	112 mm
Compression ratio	8.2:1
Number of valves	2
Intake valve opening	4° CA before TDC
Intake valve closing	54° CA after BDC
Exhaust valve opening	64° CA before BDC
Exhaust valve closing	21° CA after TDC

The CT scan of the cylinder head aimed at replicating the geometry of the intake port so as to properly obtain the intake charge flow movement as it plays a significant role in the resulting combustion process [13]. The domain encapsulates the fluid from the intake port to the exhaust port, as generally modeled for internal combustion engines (ICE) [14]. The resulting computer aided design (CAD) geometry, displayed in Fig. 1, was meshed using the fully automated grid generation module AVL FAME™ M [15] providing an unstructured dynamic mesh dominated by polyhedral cells. Depending on the moment in the engine cycle, ports are removed from the mesh when the corresponding valves are closed, to save computing resources. Local refinements were applied by the software algorithm according to in-cylinder flow near the valve and spark plug regions during their respective occurrences.

The resulting mesh, shown in Fig. 2, exhibited a global cell size of 1.5mm in agreement with current literature practice [16]. The boundary layer resolution was set with two-layer polyhedral cells having a thickness of 0.2 mm to capture near-wall effects. Valve region refinement resulted in mesh size ranging from 0.5 mm, close to the crevices (similarly to [17]), to 1 mm at more distant regions. The development of the kernel flame is captured by a 3 mm radius sphere having 0.25 mm cells at the spark-ignition location as performed in [18]. An additional region of refinement is added to take into consideration the direct injection

of EGR. To do so, EGR tubes are added to the cylinder head (see Fig. 1 and Fig. 2) and are meshed, to resolve the incoming high-speed gas, with cell size of 0.4 mm following mesh resolution recommended by [13]. This refinement level was also used in a conical region located at each tube outlet feeding the cylinder as depicted in Fig. 2. This conical refined region is activated during the EGR injection period to properly resolved the incoming EGR jet. For that reason, the entire geometry resulted in a mesh having a maximum cell count of 1,500,000 during injection and a minimum of 300,000 near top dead center, which is in the range of current practice (see [18][19], for example).

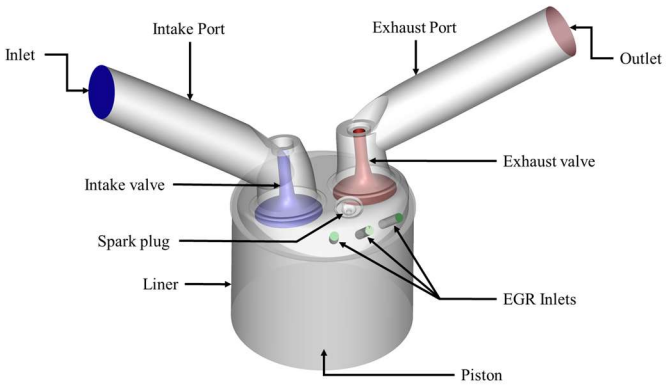

Figure 1. Computational domain of the engine.

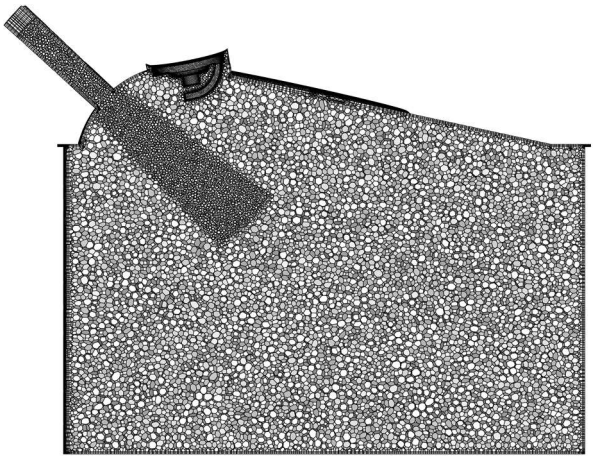

Figure 2. Computational mesh at injection timing.

B. Numerical Modeling

In this study, in-cylinder flow simulations are based on a Reynolds averaged Navier Stokes (RANS) approach using AVL FIRE™ M software [15]. The numerical method is based on the finite volume procedure to solve the discretized compressible transport equations. Pressure-velocity coupling is dealt by the Pressure Implicit with Splitting of Operators (PISO) algorithm [14]. Linear solver Algebraic Multigrid (AMG) is adopted to solve the continuity equation whereas conjugate gradient methods with preconditioner are used with the energy, species and momentum transport equations [14]. Time step size was set at 0.125°CA and 0.5°CA during combustion and valve openings/closings respectively while a constant time step of 1°CA was defined elsewhere in the cycle.

1) Turbulence Model

The turbulent flow is described using the *k–ζ–f* eddy viscosity model developed by Hanjalić, et al. [20]. This model aims to solve a transport equation by introducing a normalizing velocity scale $\zeta=\frac{\bar{v}^2}{k}$. A hybrid wall treatment is used for turbulence properties and temperature [15][20]. The *k–ζ–f* model has been validated with in-cylinder flow in the literature [21]. The kinematic turbulent eddy viscosity is represented by (1) while transport equations for the turbulent kinetic energy, *k,* its dissipation rate, ε, and the normalized velocity variable, ζ, are computed using (2) to (4), respectively [15].

$$\nu_t = C_\mu \zeta \frac{k^2}{\varepsilon} \tag{1}$$

$$\frac{Dk}{Dt} = (P_k - \varepsilon) + \frac{\partial}{\partial x_j}\left[\left(\nu + \frac{\nu_t}{\sigma_k}\right)\frac{\partial k}{\partial x_j}\right] \tag{2}$$

$$\frac{D\varepsilon}{Dt} = \frac{C^*_{\varepsilon 1} P_k - C_{\varepsilon 2}\varepsilon}{T} + \frac{\partial}{\partial x_j}\left[\left(\nu + \frac{\nu_t}{\sigma_\varepsilon}\right)\frac{\partial \varepsilon}{\partial x_j}\right] \tag{3}$$

$$\frac{D\zeta}{Dt} = f - \frac{\zeta}{k}P_k + \frac{\partial}{\partial x_j}\left[\left(\nu + \frac{\nu_t}{\sigma_\zeta}\right)\frac{\partial \zeta}{\partial x_j}\right] \tag{4}$$

2) Combustion Model

The combustion process uses the 3-Zones Extended Coherent Flame Model (ECFM-3Z) based on the description of the mixing state and the reaction progress variable [15][22]. This model relies on a three-zone cell decomposition structured by a progress variable. Such a description is inherited from the mixing nature of the turbulent flow: the fuel and the oxidizer formed two distinct zones, and are blended into a new mixing one. Thus, each computational cell is defined into three regions: an air zone that can be combined with residual gases, a pure fuel zone and an air-fuel mixing zone. The combustion model's approach is built on solving the transport equation for the flame surface density, Σ. Finally, the spark ignition is modeled with a spherical time delay model while the release of a spherical flame kernel at the spark location initiates the combustion with a predefined value of the flame surface density [15].

3) Boundary Conditions

The temperature-based boundary conditions were set according to the literature [13][17] having a similar engine load. Hence, the following surface temperatures were prescribed as follows: intake port: 375K; intake valve: 372K; engine head: 465K; cylinder liner: 430K; piston: 510K; exhaust valve: 505K; and exhaust port: 500K. Open boundaries (see Fig. 1), such as the inlet of the intake port was set to a pressure of 75kPa at 305K while the exhaust port used an outlet static pressure of 121kPa. Evaporated fuel was introduced at the inlet with a stoichiometric ratio. Gasoline is represented by a single component, octyl (C_8H_{17}). When EGR injection is activated, nitrogen (N_2) is used in lieu of burnt gases for simplicity and because this approach was used experimentally. Moreover, measured intake and exhaust valve lift profiles were incorporated into the model. Simulation starts at exhaust valve opening, as recommended by the software manual, and as such the domain (cylinder and

exhaust port) was initialized using exhaust gas at exhaust port pressure.

III. MODEL VALIDATION

Validation of the numerical model was carried out using experimental average cylinder pressure and heat release rate at 2500 rpm with a stoichiometric air-fuel ratio and an indicated mean effective pressure of 520 kPa. A spark timing of 37 deg before TDC (top dead center) was set as in the experiment. The experimental pressure curve was averaged over 400 cycles. Numerical results were extracted from the third engine cycle as more cycle demonstrated little cycle-to-cycle variations which in agreement with literature practice where between the first [23] and up to the fourth [17] engine cycle is used. The simulated and experimental curves of in-cylinder pressure and heat release rate are shown in Fig. 3.

The simulated pressure curve demonstrates an excellent overall approximation to the average experimental data. The heat release rate underlines a difference in the modeled combustion process. The combustion seems to be slightly delayed in the simulations before reaching a higher value. Nevertheless, the model is judged satisfactory as these differences are also reported in the literature for SI engines and can be explained by factors such as the use of a homogeneous charge of air and gasoline, the reduced kinetic mechanism, constant boundary conditions and other sub-model's uncertainties [24].

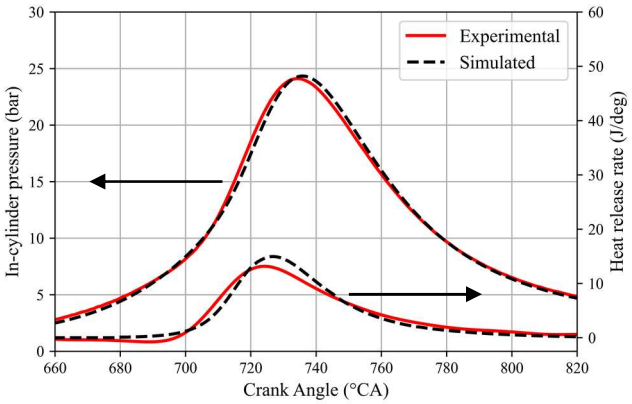

Figure 3. In-cylinder pressure and heat release rate comparison.

IV. RESULTS

Nitrogen was introduced into the cylinder in two ways: homogeneously via the intake port and stratified via three injection nozzles aiming at the cylinder center. In both cases, the same total amount of N_2 was reached, i.e., 14% of in-cylinder total mass at 2500 rpm while a 37 deg. bTDC spark timing is used. In the homogeneous case, N_2 was introduced at the inlet condition during the intake stroke as it is traditionally done. However, the homogeneous EGR results considered herein are very similar to the validation case (named 'base case' hereafter) and as such are not shown in what follows for brevity. For the stratified case, N_2 was injected starting at bottom dead center under subsonic conditions. The injection duration and mass-flow profiles were defined based on experimental conditions and the valve manufacturer's data sheet. Thus, a trapezoidal mass-flow profile was chosen to mimic the injection behavior such as the transient opening and closing of the valve and its nominal flow rate.

Timing	Figure
Halfway through the injection (140deg bTDC)	
End of injection (100 deg bTDC)	
Halfway between the end of the injection and spark timing (70 deg bTDC)	
At spark timing (37 deg bTDC)	

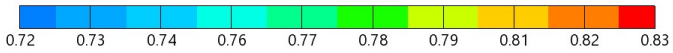

Figure 4. N_2 mass fraction distribution and velocity vectors as a function of crank angle degree.

The analysis begins by illustrating how stratification is achieved due to N_2 direct injection. Fig. 4 illustrates, at different times, the N_2 mass fraction concentration above the average in-cylinder N_2 level so as to identify the stratification structure. Velocity vectors are also displayed to illustrate flow direction. Fig. 4, top, illustrates the impact of the injected N_2 on both the liner and piston surfaces at halfway through the injection process. The N_2 jet is deflected by the surfaces and propagates in every direction evenly as displayed by the uniform vectors and the circular distribution of the mass fraction. Fig. 4, second image from the top, shows a N_2 stratification obtained by the N_2 jet movement around the cylinder periphery at the end of the injection (100 deg bTDC). The development of N_2 flow is

greatly influenced, as observed by the velocity vector orientation, by 1) the position of the EGR tubes, which aim at the opposite side of the cylinder resulting in jet deflection and 2) the movement of the piston that tends to push N_2 toward the cylinder head. Fig. 4, third image from the top, is set halfway between the end of the N_2 injection and spark timing. It shows the presence of a circular motion on the left side of the cylinder that dives toward the piston in the vicinity of the EGR inlets and goes through an upwards movement on the right side. As the compression stroke follows its course, the stratification level decreases as can be observed in the bottom image of Fig. 4 where the N_2 mass fraction distribution is shown at spark timing. One now observes that at ignition, a higher concentration of N_2 is located along the cylinder liner and that the maximum concentration is lower due to mixing by the turbulent flow. High N_2 concentration at spark location is avoided as the stratification remains along the liner surfaces of the engine.

To gain a better understanding at the influence of N_2 direct injection and its resulting turbulence generation, if any, the average turbulent kinetic energy (TKE) within the cylinder is now analyzed. TKE was also used by Millo et al. [25] to describe the turbulence level of in-cylinder flow. Fig. 5 displays the significant impact of N_2 direct injection on the turbulence inside the engine cylinder and allows comparing the behavior with the case in absence of EGR. It is worth noticing that TKE of the base case is in good agreement with other engine studies [23][25]. Fig. 5 shows that in the absence of direct injection, TKE peaks at the maximum intake valve lift, denoting the strong contribution of the intake flow to the cylinder turbulence. It also shows that the injection process (green zone) contributed to the increase of TKE after several crank angle degrees following the beginning of the injection, which is linked to the trapezoidal mass-flow profile. Moreover, TKE peaks when the nominal flow rate is reached. The resulting increase of TKE due to the injection process has the benefit to last until the spark timing at which time TKE is twice as high as the cases without EGR (see Fig. 5). Therefore, the increase of TKE is expected to induce a flame speed increase during combustion under the assumptions of a fully isentropic and homogeneous turbulent flow field [26].

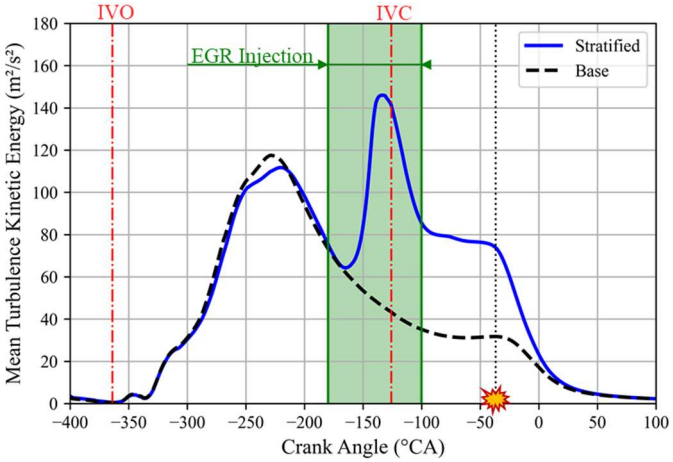

Figure 5. Turbulent kinetic energy plot for the base and stratified cases.

Following TKE quantification, the turbulent intensity (TI) at spark timing is analyzed so as to further quantify the influence of N_2 direct injection on the resulting flow. TI is defined by the root mean square (rms) of velocity fluctuations, *u'*, normalized by the mean piston speed. Fig. 6 compares TI distribution along two perpendicular axes for the base case (thus, without EGR) (top) and with N_2 injection (bottom). It can be noticed that the injection resulted in a significant turbulent intensity increase of 55%, especially in the center region of the cylinder and thus, in the vicinity of the spark plug. A twofold increase in maximum TI value is observed when comparing each case.

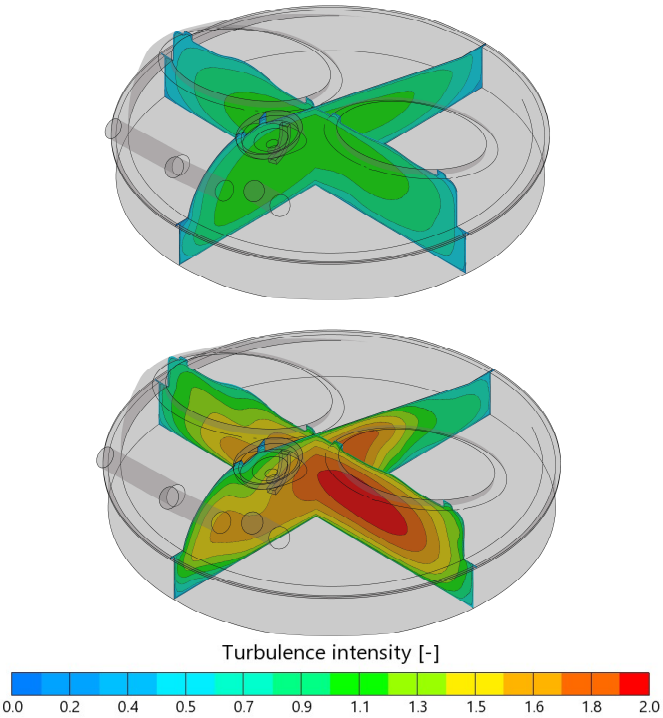

Figure 6. Contours of turbulent intensity (u' over piston speed) of base case (top) and injection case (bottom) at spark ignition (same scale).

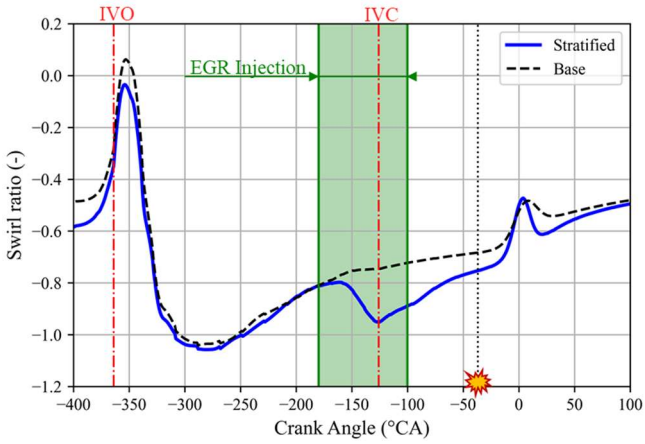

Figure 7. Swirl ratio for the base and stratified cases

Finally, the consequence of injecting N_2 directly in the cylinder on the tumble and swirl ratios is characterized. First, it is noted that, based on the CFD simulations, the tumble ratio is very low for most of the engine cycle thus, the results are not shown as it probably played no significant role in the turbulence intensity for this engine. However, the engine possesses a

negative swirling flow that decreases in intensity during the compression stroke, as expected, and shown in Fig. 7 for the base case. However, for the stratified direct injection of N_2, an increase in swirling motion intensity by nearly 30% is observed and the higher swirl ratio persists until after spark ignition. Increasing swirl intensity in SI engine is known to increase flame propagation and stability [27] and therefore, this could be a benefit of the configuration evaluated herein of the proposed technology.

V. CONCLUSIONS

Stratified EGR is a technique that has been studied over the years as a way to increase the amount of burnt gas in the cylinder before the appearance of its negative impact on combustion. Herein, a novel approach is proposed and consisted in directly injecting EGR in the cylinder by passing through the cylinder head. Based on a proof of concept, a 3D CFD model has been developed with the objective of characterizing how the direct injection of gas in the cylinder would impact stratification and turbulence. The latter is known to increase flame speed.

The CFD results showed a clear radial distribution of nitrogen along the cylinder liner confirming stratification. Moreover, one advantageous consequence of achieving EGR stratification through direct injection is that it increased turbulence as characterized by turbulent kinetic energy, turbulence intensity, and swirl ratio. In upcoming paper, further analysis will assess the impact on the combustion process.

ACKNOWLEDGMENT

The authors would like to acknowledge the financial support of the National Sciences and Engineering Research Council of Canada (NSERC) discovery grant. The CFD software was provided by AVL List GmbH thanks to the University Program Partnership (UPP).

REFERENCES

[1] L. Fridstrøm, "From innovation to penetration : calculating the energy transition time lag for motor vehicles," *Energy Policy*, vol. 108, pp. 487-502, 2017.

[2] F. Duronio, A. De Vita, A. Montanaro and C. Villante, "Gasoline direct injection engines – A review of latest technologies and trends. Part 2," *Fuel*, vol. 265, no. 116947, 2020.

[3] C. Pardhi, R. Prasad, C. P. Jawahar, S. Chhalotre and Z. Said, "Review on performance and emission of spark ignition engine using exhaust gas recirculation," *Energy Sources, Part A: Recovery, Utilization and Environmental Effects*, vol. 45, no. 2, pp. 3692-3707, 2023.

[4] M. Dong, G. Chen, M. Xu and C. Daniels, "A Preliminary CFD investigation of in-cylinder stratified EGR for spark ignition engines," *SAE Technical Paper 2002-01-1734*, 2002.

[5] W. N. Groves and M. Bjorkhaug, "Stratified exhaust gas recirculation in a S.I. engine," *SAE Technical Paper 860318*, 1986.

[6] J. Stokes, T. H. Lake, M. J. Christie and I. Denbratt, "Improving the NOx/fuel economy trade-off for gasoline engines with the CCVS," *SAE Technical Paper 940482*, 1994.

[7] T. H. Lake, J. Stokes, K. J. Pendlebury and I.Denbratt, "Development experience of a multi-cylinder CCVS engine," *SAE Technical Paper 950165*, 1995.

[8] N. S. Jackson, J. Stokes, T. H. Lake, S. M. Sapsford, M. Heikal and I. Denbraft, "Understanding the CCVS stratified EGR combustion system," *SAE Technical Paper 960837*, 1996.

[9] S. Han and W. K. Cheng, "Design and demonstration of a spark ignition engine operating in a stratified-EGR mode," *SAE Technical Paper 980122*, 1998.

[10] M. Ditiu, "Triple stratification in a spark ignition engine : the effect on the emission at unthrottled light load," *SAE Technical Paper 1999-01-0575*, 1999.

[11] F. Sarikoc, M. Kettner, A. Velji, U. Spicher, A. Krause and A. Elsaesser, "Potential of reducing the NOX emissions in a spray guided DI gasoline engine by stratified exhaust gas recirculation (EGR)," *SAE Technical Paper 2006-01-1261*, 2006.

[12] Y. Woo, K. Yeom, C. Bae, S. Oh and K. Kang, "Effects of stratified EGR on the performance of a liquid phase LPG injection engine," *SAE Technical Paper 2004-01-0982*, 2004.

[13] S. Sahoo and D. K. Srivastava, "Numerical analysis of performance, combustion, and emission characteristics of PFI gasoline, PFI CNG, and DI CNG engine," *Energy*, vol. 278, no. 127749, 2023.

[14] M. Thelliez, A. Ennemoser, M. I. Segura and K.-K. Lee, "CFD methodology for greenhouse gas emissions reduction," *MTZ Worldwide*, vol. 81, no.11, pp. 50-55, 2020.

[15] AVL List GmbH, "AVL FIRE™ M, User Manual", 2024.

[16] Y. Yan, R. Yang, X. Sun, R. Li and Z. Liu, "Numerical investigations of injection timing effects on a gasoline direct injection engine performance : Part A, in-cylinder combustion process," *Frontiers in Energy Research*, vol. 10, no. 828167, 2022.

[17] S. K. Gupta and M. Mittal, "A CFD study on the effect of compression ratio on combustion characteristics and emissions in a spark-ignition engine," *Progress in Computational Fluid Dynamics*, vol. 20, no. 5, pp. 299-306, 2020.

[18] G. G. Gianetti, T. Lucchini, G. D'Errico, A. Onorati and P. Soltic, "Development and validation of a CFD combustion model for natural gas engines operating with different piston bowls," *Energies*, vol. 16, no. 2, 2023.

[19] S. Sahoo, S. Tripathy and D.K. Srivastava, "Numerical investigation on the effect of EGR in a premixed natural gas SI engine," in *Proceedings of the 7th International Conference on Advances in Energy Research*, M. Bose and A. Modi, Eds. Singapore: Springer, 2021, pp. 1477-1487.

[20] K. Hanjalić, M. Popovac and M. Hadžiabdić, "A robust near-wall elliptic-relaxation eddy-viscosity turbulence model for CFD," *International Journal of Heat and Fluid Flow*, vol. 25, no. 6, pp. 1047-1051, 2004.

[21] S. Saric, B. Basara, K. Suga and S. Gomboc, "Analytical wall-function strategy for the modelling of turbulent heat transfer in the automotive CFD applications, *SAE Technical Paper 2019-01-0206,* 2019"

[22] O. Colin and A. Benkenida, "The 3-zones extended coherent flame model (Ecfm3z) for computing premixed/diffusion combustion," *Oil & Gas Science and Technology*, vol. 59, no. 6, pp. 593-609, 2004.

[23] I. Verma, E. Bish, M. Kuntz, E. Meeks, K. Puduppakkam, C. Naik and L. Liang, "CFD modeling of spark ignited gasoline engines- Part 1: modeling the engine under motored and premixed-charge combustion mode," *SAE Technical Paper 2016-01-0591*, 2016.

[24] J. Liu, J. Szybist and C. Dumitrescu, "Choice of tuning parameters on 3D IC engine simulations using G-equation," *SAE Technical Paper 2018-01-0183*, 2018.

[25] F. Millo, S. Luisi, F. Borean and A. Stroppiana, "Numerical and experimental investigation on combustion characteristics of a spark ignition engine with an early intake valve closing load control," *Fuel*, vol.121, pp. 298-310, 2014.*Technical Paper 2016-01-0591*, 2016.

[26] M. Sjeric, J. Krajnovic and A. Vučetic, "Influence of swirl flow on combustion and emissions in spark-ignition experimental engine," *Journal of Energy Engineering* , vol. 147, no. 4, 2021.

[27] J. B. Heywood, Internal Combustion Engine Fundamentals, 2nd ed. New York: McGraw-Hill Education, 2018, pp. 36